Journal of Inorganic Biochemistry 105 (2011) 149–154

Contents lists available at ScienceDirect

Journal of Inorganic Biochemistry

journal homepage: www.elsevier.com/locate/jinorgbio

Studies on synthesis, characterization, and G-quadruplex binding of Ru(II) complexes containing two dppz ligands

Jing Sun [a,b], Yan An [c], Li Zhang [a], Huo-Yan Chen [a], Yan Han [a], Yu-Jia Wang [a], Zong-Wan Mao [a,*], Liang-Nian Ji [a,*]

[a] MOE Key laboratory of Bioinorganic and Synthetic Chemistry, School of Chemistry and Chemical Engineering, Sun Yat-Sen University, Guangzhou, 510275, China
[b] School of Pharmacy, Guangdong Medical College, Dongguan, 523808, China
[c] Institute of Marine Materials Science and Engineering, Shanghai Maritime University, Shanghai 201306, China

ARTICLE INFO

Article history:
Received 13 July 2010
Received in revised form 2 October 2010
Accepted 6 October 2010
Available online 14 October 2010

Keywords:
Synthesis
Ru(II) complex
dppz
G-quadruplex

ABSTRACT

In this work, the interaction between the guanine-rich single-strand oligomer $AG_3(T_2AG_3)_3$ quadruplex and two Ru(II) complexes, $[Ru(L^1)(dppz)_2](PF_6)_4$ (1) and $[Ru(L^2)(dppz)_2](PF_6)_4$ (2) (L^1 = 5,5′-di(1-(trimethylammonio) methyl)-2,2′-dipyridyl cation, L^2 = 5,5′-di(1-(triethylammonio)methyl)-2,2′-dipyridyl cation, dppz = dipyrido [3,2-a:2′,3′-c] phenazine), has been studied by UV–Visible, fluorescence, DNA melting, and circular dichroism in K^+ buffer. The two complexes after binding to G-quadruplex have shown different DNA stability and fluorescence enhancement. The results show that both complexes can induce the stabilization of quadruplex DNA. ΔT_m values of complexes 1 and 2 at [Ru]/[DNA] ratio of 1:1 were 9.4 and 7.0, respectively. Binding stoichiometry along with the quadruplex was investigated through a luminescence-based Job plot. The major inflection points for complexes 1 and 2 were 0.49 and 0.46, respectively. The data were consistent with the binding mode at a [quadruplex]/[complex] ratio of 1:1. In addition, the conformation of G-quadruplex was not changed by the complexes at the high ionic strength of K^+ buffer.

1. Introduction

Guanine-rich sequences of DNA have the propensity to form tetraplex structures known as G-quadruplexes [1–4]. During the past decade, these G-quadruplexes have received great attention because they can inhibit telomere extension by telomerase, which is an enzyme in over 80% cancer cells [5–7]. This unique activity of telomerase makes the enzyme an ideal probe for tumor diagnosis and a target for cancer chemotherapy [8,9]. Molecules, which have (a) a π-delocalized system, (b) a partial positive charge in the center of the molecular scaffold, and (c) a positively charged substituent to interact with the grooves, loops, and the negatively charged phosphate backbone, most likely interact with and further stabilize G-quadruplexes [10]. Therefore, many research groups have designed and synthesized some molecules with such structures, which are believed to be able to interact with G-quadruplex DNA structures. This interaction plays an important role to maintain the telomeres [11–15]. Furthermore, inducement/stabilization features of G-quadruplex structures by small molecules directly prevent elongation of telomeres by disrupting the interaction between the enzyme and its substrate. A number of transition metal complexes have been designed to target quadruplex DNA. These complexes generally have positively charged substituents, which can interact with the grooves of the quadruplex, and a positively charged center, which can stay near the center of the guanine quartet. The metal plays a major structural role in organizing the ligand(s) into an optimal structure for quadruplex DNA interaction [16–19]. Also, the electropositive metal is in principle positioned at the center of the guanine quartet and increases electrostatic stabilization by substituting the cationic charge of the potassium or sodium that normally occupies this site.

Ru(II) complexes have prominent DNA-binding properties, especially the complex $[Ru(bpy)_2(dppz)]^{2+}$ (dppz = dipyrido[3,2-a:2′,3′-c] phenazine) known as DNA "light switch". The complex can intercalate between the duplex DNA base pairs and stabilize the DNA [20–22]. Shi, et al. have studied the action of $[Ru(bpy)_2(dppz)]^{2+}$ with 5′-AGGGTTAGGGTTAGGGTTAGGG-3′ ($AG_3(T_2AG_3)_3$) and 5′-CCCTAACCC-TAACCCTAACCCT-3′ and found that the complex can serve as a prominent molecular "light switch" for both G-quadruplexes. It prefers to bind to G-quadruplexes induced by either Na^+ or K^+ over an i-motif [23]. As a star molecule, it would consist of one dppz ligand and two ancillary ligands. However, the complex combined with two dppz ligands is rare. Herein, we studied the interaction of two complexes of $[Ru(L^1)(dppz)_2](PF_6)_4$ (1) and $[Ru(L^2)(dppz)_2](PF_6)_4$ (2) (L^1 = 5,5′-di (1-(trimethylammonio)methyl)-2,2′-dipyridyl cation; L^2 = 5,5′-di(1-(triethylammonio)methyl)-2,2′-dipyridyl cation) and G-quadruplexes. The synthetic route and structure of complex 2 are shown in Scheme 1.

* Corresponding authors. Tel.: +86 20 8411 3788; fax: +86 20 8411 2245.
E-mail addresses: cesmzw@mail.sysu.edu.cn (Z.-W. Mao), cesjln@mail.sysu.edu.cn (L.-N. Ji).

0162-0134/$ – see front matter © 2010 Elsevier Inc. All rights reserved.
doi:10.1016/j.jinorgbio.2010.10.005

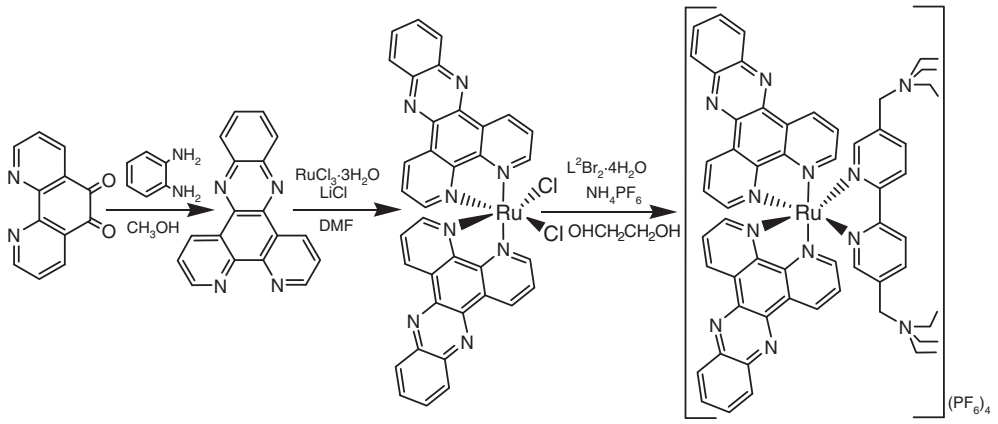

Scheme 1. The synthetic route of complex 2.

2. Experimental section

2.1. Materials

DNA oligomers $AG_3(T_2AG_3)_3$ were purchased from Sangon (Shanghai, China) and used without further purification. Concentrations of these oligomers were measured through the absorbance at 260 nm of melted samples. Single-strand concentrations were spectroscopically determined and calculated by using the molar absorption coefficient of quadruplex, $\varepsilon = 2.16\times10^5\ M^{-1}\ cm^{-1}$(per quadruplex) at 260 nm for G-quadruplex [24]. The formation procedure of intramolecular G-quadruplexes was carried out as follows. An oligonucleotide sample dissolved in a buffer solution was heated to 90 °C for 5 min. The solution was slowly cooled down to room temperature and then incubated at 4 °C overnight. The buffer solution was composed of 100 mM KCl, 10 mM KH_2PO_4/K_2HPO_4, and 1 mM K_2H_2EDTA with A pH of 7.0. All reagents and solvents were purchased commercially and used without further purification unless specially noted. Doubly distilled water was used to prepare buffer solutions.

2.2. Physical measurement

Elemental analyses (C, H, and N) were carried out with a Perkin-Elmer 240 C elemental analyzer. ^{1}H NMR spectra were recorded on a Varian Mercury-plus 300 NMR spectrometer with DMSO-*d*6 as a solvent and $SiMe_4$ as an internal standard at 300 MHz at room temperature. Electrospray ionization mass spectrometry (ESI-MS) was recorded on a LQC system (Finngan MAT, USA) using CH_3CN as a mobile phase. UV–Visible (UV–Vis) and emission spectra were recorded on Perkin-Elmer Lambda-850 spectrophotometer and Ls55 spectrofluorophotometer. The circular dichroism (CD) spectra were recorded on a Jasco J-810 spectropolarimeter.

2.3. Preparation of ligands and complexes

5,5′-Dimethyl-2,2′-dipyridyl was purchased from Aldrich Chemical Co. 5,5′-Dibromomethyl-2,2′-dipyridyl, L^1Br_2 and $L^2Br_2\cdot4H_2O$ were synthesized and characterized according to our previous method [25,26]. The compounds of 1,10-phenanthroline-5,6-dione [27], dppz [28], *cis*-$[Ru(dppz)_2Cl_2]\cdot2H_2O$ [29], and complex 1 [30] were prepared and characterized according to methods in the literature.

2.3.1. $[Ru(L^2)(dppz)_2](PF_6)_4\cdot CH_3OH\cdot1.25H_2O\cdot1.5CH_3CN$ (2)

A solution of *cis*-$[Ru(dppz)_2Cl_2]\cdot2H_2O$ (0.26 g, 0.34 mmol) and $L^2Br_2\cdot4H_2O$ (0.21 g, 0.34 mmol) in ethylene glycol (30.0 cm^3) was heated at 130 °C under the protection of argon for 6 h. In the process, the solution turned dark red. The solution was cooled down to room temperature and filtrated. Saturated NH_4PF_6 was added dropwise to the solution and red–orange precipitate, which was filtered and recrystallized with CH_3CN/CH_3OH (1:1, v/v), was obtained. The yield of the product was 0.27 g (47%). The atom weight fractions of the stoichiometric molecule of $C_{128}H_{141.50}F_{48}N_{27}O_{4.50}P_8Ru_2$ (3492.08) are as follows: C of 44.03%, H of 4.08%, and N of 10.83%. The analytical value of the atom weight fractions were C of 44.01%, H of 4.10%, and N of 10.80%. The ESI-MS spectra were analyzed at *m/z* 1484.9 $[M\text{-}PF_6]^+$ (60), 670.5 $[M\text{-}2PF_6]^{2+}$ (100), and 398.5 $[M\text{-}3PF_6]^{3+}$ (25). ^{1}H NMR (DMSO-*d*6), $\delta = 9.74$ (dd, 2 H), 9.62 (dd, 2 H), 9.10 (d, 2 H), 8.51 (m, 6 H), 8.30 (d, 2 H), 8.22 (d, 2 H), 8.12 (m, 6 H), 7.79 (d, 2 H), 7.90 (s, 2 H); 4.34 (s, 4 H), 2.99 (q, 12 H), 1.00 (t, 18 H).

2.4. X-ray crystallography

Single crystal X-ray diffraction (XRD) experiments were carried out with a Bruker Smart Apex CCD area detector at 173(2) K for complex 2. The dimensions of the crystal of complex 2 used for X-ray diffraction analysis were $0.48\times0.30\times0.21$ mm. XRD pattern was recorded with Mo Kα radiation ($\lambda = 0.71073$ Å). The data were collected in the θ range of 1.79–25.00°. Total 57149 independent reflections were obtained, and 27,464 reflections with $|F_o| \geq 2\sigma(F_o)$ were used for the further calculations. Absorption corrections were applied by the SADABS program [31]. The structure was analyzed by direct methods. All non-hydrogen atoms were refined anisotropically by least-squares on *F*2 using the SHELXTL program [32]. These were refined isotropically first and then anisotropically. The hydrogen atoms of the ligands were placed in calculated positions with fixed isotropic thermal parameters and the structure factors of calculation were included in the final stage of full-matrix least-squares refinement. The final discrepancy factors were $R_1 = \sum||F_o| - |F_c||/\sum|F_o| = 0.1086$ and $wR_2 = [\sum w(F_o^2 - F_c^2)^2/\sum w(F_o^2)^2]^{1/2} = 0.2374$ with weight $w = 1/[\sigma^2(F_o^2) + (0.0410\ P)^2 + 83.4000\ P]$ where $P = (F_o^2 + 2F_c^2)/3$. The crystal data is summarized in Table 1.

2.5. Absorption and emission spectra

The absorption and emission spectra as well as titration curves were recorded through a constant concentration of complexes, to which the DNA stock solution were added step by step at room temperature. The concentrations of the $[Ru(L)(dppz)_2]^{4+}$ solution were 10.0 μM and 2.0 μM, and the volume of the complex was 3000 μL. Complex-DNA solutions were incubated for 5 min before absorption spectra were recorded. The titration processes were repeated several times until no change was observed in the spectra. It indicated that binding saturation was achieved. The changes in the

Table 1
Crystallographic data of complex 2.

Complex	$(2\cdot CH_3OH\cdot 1.25H_2O\cdot 1.5CH_3CN)\times 2$
Empirical formula	$C_{128}H_{141.50}F_{48}N_{27}O_{4.50}P_8Ru_2$
Formula weight	3492.08
Temperature (K)	173(2)
Wavelength (Å)	0.71073
Crystal system, Space group	Triclinic, *P-1*
a (Å)	20.094(3)
b (Å)	21.299(3)
c (Å)	22.377(3)
α/°	108.560(2)
β (°)	114.511(2)
γ/°	97.221(2)
Volume (Å^3)	7883.4(2)
Z	2
D_{calcd} (g cm^{-3})	1.471
F(000)	3549
Crystal size (mm)	0.48×0.30×0.21
θ range for data collection (°)	1.79 to 25.00
Limiting indices	$-23\le h\le 23$, $-25\le k\le 25$, $-25\le l\le 25$
Reflections collected	57,149
Independent reflections	27,464 ($R_{int}=0.0516$)
Goodness-of-fit on F^2	1.045
R_1/wR_2 [$I>2\sigma(I)$][a]	0.1086/0.2374
R_1/wR_2 (all data)	0.1893/0. 2803
Largest diff. peak (eA^{-3})	1.340/−0.953

Ru(II) complex concentration caused by dilution at the end of each titration were negligible.

2.6. Thermal denaturation of DNA

Thermal denaturation of DNA was carried out with a PerkinElmer Lambda 850 spectrophotometer equipped with a Peltier temperature-control programmer (±0.1 °C). The temperature of the solution was increased from 40 to 90 °C at a rate of 1 °C min^{-1}, and the absorbance at 295 nm was continuously monitored for solutions of DNA (10.0 μM) in the absence and presence of the Ru(II) complex (10.0 μM). The data were presented as $(A-A_f)/(A_0-A_f)$ vs. temperature, where A, A_f and A_0 were the observed absorbances at temperature T, at 90 °C, and at 40 °C, respectively, at 295 nm.

2.7. Continuous variation analysis

Binding stoichiometries were obtained for the two complexes using the method of continuous variation [33,34]. The concentrations of both metal complexes and DNA varied, while the sum of the concentrations of the two reactants was kept constant at 10 μM. In the solutions, the mole fraction of the Ru(II) complex varied from 1 to 0 in 0.1 increments. Each mixture was equilibrated at 5 °C for 12 h in the dark. The fluorescence intensities of these mixtures were measured at 25 °C using an excitation wavelength of 446 and 449 nm for complexes 1 and 2, respectively. The F_{max} (fluorescence) was recorded in the range of 500–750 nm. Binding stoichiometries were obtained from the intercepts of the linear plot obtained by linear least-squares fits to the left- and right-hand portions of the Job plots.

2.8. Circular dichroism measurements

CD titration procedure was described as follows: 4.0 μL Ru(II) (200 μM) complex was added sequentially to solutions containing G-quadruplex (5.0 μM). All solutions were mixed thoroughly and allowed to equilibrate for 5 min before data collection. The titration process was repeated several times until no change was observed. It indicated that binding saturation was achieved. For each sample, the spectrum was scanned at least three times and accumulated over the wavelength range of 200–350 nm at a temperature of 25 °C. The spectrum of the buffer was subtracted from the average spectrum for each sample.

3. Results and discussion

Fig. 1 depicts the structure of complex 2. Selected bond distances and bond angles of complex 2 are listed in Table 2. The complex molecule contains a six-coordinated ruthenium atom chelated by one dicationic L ligand and two dppz ligands. The coordination geometry of the ruthenium atom is a distorted octahedron with a mean bite angle of 79.67° over three bidentate ligands. The mean Ru–N bond length of 2.061 Å is typical for six-coordinated Ru(II) complexes, which is similar to complex 1 [30].

Titration was performed to determine the binding affinity of the complexes to G-quadruplex. The DNA sample was added sequentially to complex solutions. The absorbance spectra were recorded after each addition. The changes in the spectral profiles during titration are shown in Fig. 2. The absorbance in the ligand absorption region, as well as the MLCT (metal-to-ligand charge transfer) band, decreased with increasing concentration of DNA. The hypochromisms ($H\%$), defined as $H\% = 100\%\cdot(A_{free}-A_{bound})/A_{free}$, of MLCT bands of complexes 1 and 2, were calculated as about 17.94% and 13.33%, respectively. In order to compare the DNA-binding affinities of the two complexes quantitatively, their intrinsic DNA-binding constants K_b were obtained by monitoring the changes of the MLCT absorbance of both complexes according to Eq. (1) [35–38], where [DNA] is the concentration of DNA in nucleotides, ε_a is the molar absorption coefficient (A_{abs}/[M]) of the MLCT absorption band at a given DNA concentration, ε_f and ε_b are the molar absorption coefficients of the free Ru(II) complex and the molar absorption coefficient of the Ru(II) complex in the fully bound form, respectively. K_b is the equilibrium binding constant in M^{-1}, C_t is the total Ru(II) complex concentration, and s is the binding site size. Eq. (1) has been applied to titration data for noncooperative metallointercalator binding to DNA.

$$\left(\varepsilon_a-\varepsilon_f\right)/\left(\varepsilon_b-\varepsilon_f\right)=\left(b-\left(b^2-2K_b^2C_t[\mathrm{DNA}]/s\right)^{1/2}\right)/2K_bC_t \quad (1a)$$

$$b=1+K_bC_t+K_b[\mathrm{DNA}]/2s \quad (1b)$$

The intrinsic binding constants K_b of complexes 1 and 2 were $(9.14\pm0.47)\times10^7$ M^{-1} and $(4.50\pm0.19)\times10^7$ M^{-1}, respectively, from the decay of the absorbance (Table 3). The binding constant K_b of complex 1 is larger than that of complex 2. It indicated that complex 1 bound to the DNA more tightly than complex 2 did. The two complexes have the same intercalative ligand. This trend is mostly because of the difference between the ancillary ligands, which can be explained by the less sterical hindrance of methyl in complex 1 than

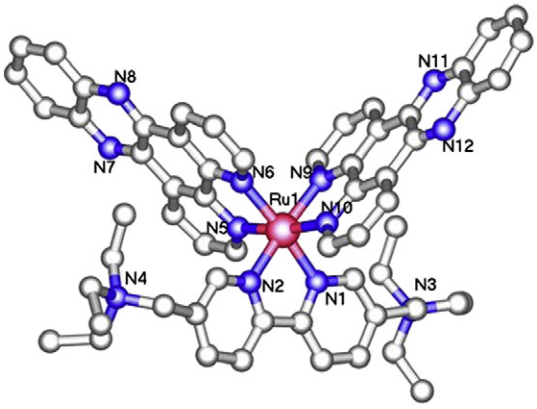

Fig. 1. X-ray crystal structure of complex 2. All the hydrogen atoms are omitted for clarity.

Table 2
Selected bond lengths (Å) and angles (°) for metal environments of complex 2.

Ru(1)–N(1)	2.057(7)	Ru(1)–N(2)	2.040(8)
Ru(1)–N(5)	2.068(9)	Ru(1)–N(6)	2.084(7)
Ru(1)–N(9)	2.059(8)	Ru(1)–N(10)	2.060(8)
N(1)–Ru(1)–N(2)	78.7(3)	N(1)–Ru(1)–N(5)	95.4(3)
N(1)–Ru(1)–N(6)	173.6(3)	N(1)–Ru(1)–N(9)	98.2(3)
N(1)–Ru(1)–N(10)	91.6(3)	N(2)–Ru(1)–N(5)	89.7(3)
N(2)–Ru(1)–N(6)	96.7(3)	N(2)–Ru(1)–N(9)	174.9(3)
N(2)–Ru(1)–N(10)	95.8(3)	N(5)–Ru(1)–N(6)	80.1(3)
N(5)–Ru(1)–N(9)	94.6(3)	N(5)–Ru(1)–N(10)	171.8(3)
N(6)–Ru(1)–N(9)	86.7(3)	N(6)–Ru(1)–N(10)	93.2(3)
N(9)–Ru(1)–N(10)	80.2(3)		

that of ethyl in complex 2. In general, the larger sterical hindrance in ancillary ligand will reduce the interaction of the complexes with DNA.

Luminescence measurements were used to further clarify the nature of the interaction between these complexes and G-quadruplex DNA. The results of the fluorescence titration for these complexes with DNA are shown in Fig. 3. Both complexes showed fluorescence in buffer solutions with a maximum wavelength of about 630 nm. The fluorescence intensity of these complexes would reach a maximum with increasing DNA concentration. The intensities at the maximum were 4.8 and 7.6 times than that in the absence of DNA for complexes 1 and 2, respectively. It is worth noting that the increasing extent of the fluorescence intensity of complex 2 is bigger than complex 1.

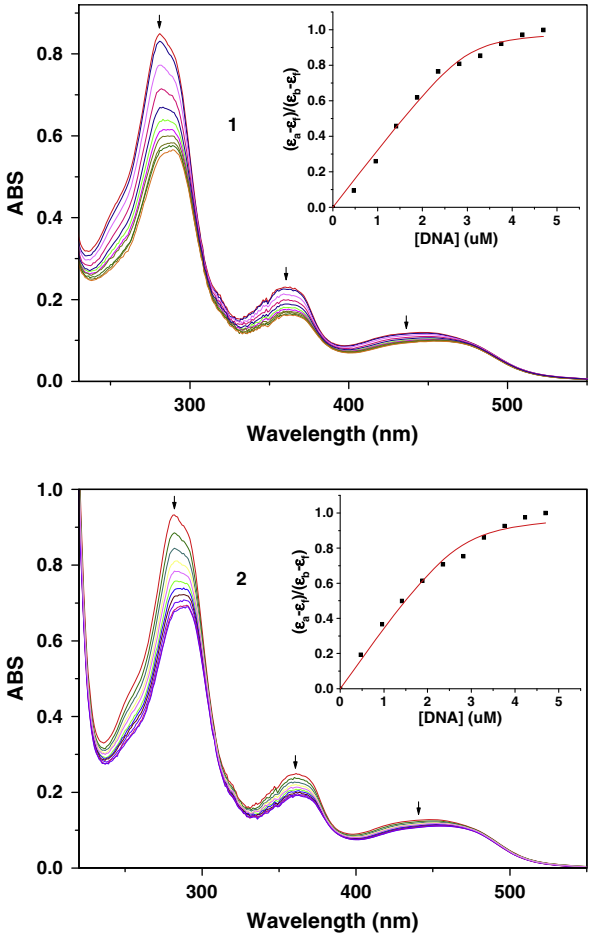

Fig. 2. Absorption spectra of complexes 1 and 2 in buffer with increasing amounts of G-quadruplex. [Ru] = 10.0 μM, [DNA] = 0–4.5 μM from top to bottom. Arrows refer to the change in absorbance upon increasing the DNA concentration. Inset: plot of $(\varepsilon_a-\varepsilon_f)/(\varepsilon_b-\varepsilon_f)$ vs. [DNA] and the nonlinear fit for the titration of DNA to Ru(II) complexes.

Table 3
Absorption spectra (λ_{max}/nm) and DNA-binding constants K_b ($\times 10^7\ M^{-1}$) of complexes 1 and 2.

Complex	λ_{max}(free)	λ_{max}(bound)	Δλ/nm	H/(%)	K_b /$10^7\ M^{-1}$	s
1	446	457	11	17.94	9.14 ± 0.47	3.19 ± 0.18
	361	359	−2	29.04		
	281	289	8	33.40		
2	449	453	4	13.33	4.50 ± 0.19	2.90 ± 0.22
	361	363	2	23.12		
	282	290	8	26.00		

Since the hydrophobic environment inside the DNA helix reduces the accessibility of solvent water molecules to the complex thus the complex mobility is restricted at the binding site, leading to the decrease of vibrational modes of relaxation [39]. This phenomenon can be explained by the hydrophilic property of the complexes. Complex 2 showed less solubility than complex 1 in water at the same condition. The property of complex 1 most likely caused the fluorescence be quenched much more easily than complex 2.

The thermal behavior of G-quadruplex DNA in the presence of complexes can provide insight into their conformational changes with the temperature and the interaction between the complexes and DNA. As shown in Fig. 4, the T_m of G-quadruplex in buffer solutions was 68.9 °C. After addition of complexes 1 and 2, the T_m of the DNA increased to 78.3 °C and 75.9 °C, respectively, at a concentration ratio [Ru]/[DNA] = 1:1. The ΔT_m values of complexes 1 and 2 were 9.4 °C and 7.0 °C, respectively. The results indicated that both complexes can

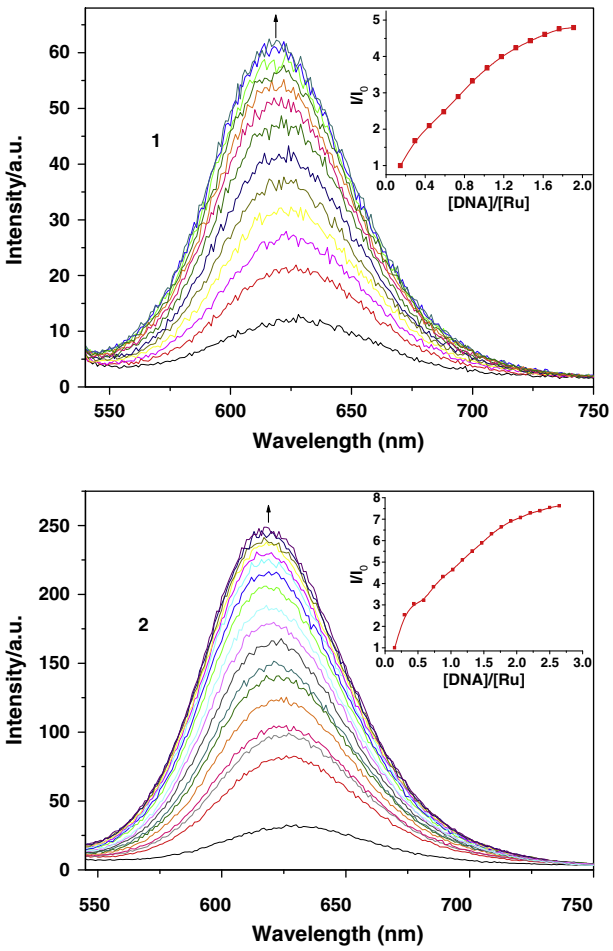

Fig. 3. Emission spectra of complexes 1 and 2 in buffer with increasing amounts of G-quadruplex, [Ru] = 2.0 μM, [DNA] = 0–5.0 μM. Arrow refers to the emission intensity changes upon increasing DNA concentrations.

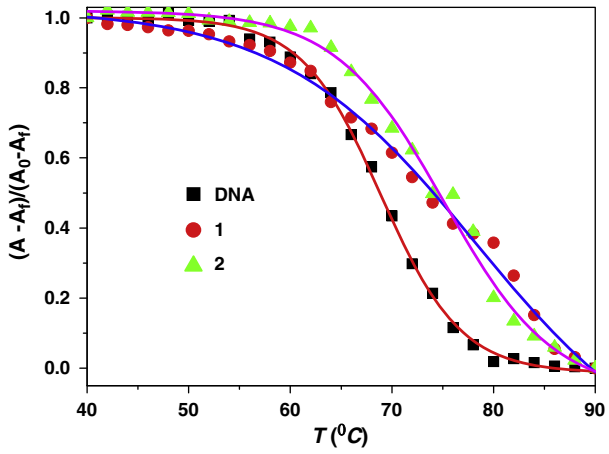

Fig. 4. Normalized UV melting curves of G-quadruplex in the absence (■) or presence of complexes 1 (●) and 2 (▲) at a [complex]/[DNA] ratio of 1:1. The absorbance was measured at 295 nm and the temperature was varied from 40 to 90 °C at a heating rate of 1 °C min^{-1}.

stabilize G-quadruplex DNA and complex 1 affected the stability of G-quadruplex more than complex 2. The difference may originate from the different DNA-binding affinity. It should be noted that the ΔT_m values of the two complexes in this work are higher than that of $[Ru(bpy)_2(dppz)]^{2+}$ [23] at the same condition. The mechanism is not clear yet, however, it is important for determining the number of dppz ligands, which enhance the stability of G-quadruplex DNA. It was reported that the telomerase inhibition activity of drugs was strongly related to the stabilization of the quadruplex structure. Therefore, both complexes might be potential anticancer drugs.

Fig. 5 shows the Job plots of the two complexes. Two major inflection points for both complexes, at $x = 0.49$ for complex 1 and at $x = 0.46$ for complex 2, were observed. These data are consistent with the binding mode at a [quadruplex]/[complex] ratio of 1:1 [24,40].

In order to determine the selectivity of the complexes for any particular G-quadruplex conformation, circular dichroism (CD) experiments were carried out. K^+ ions induce and stabilize the parallel and anti-parallel conformations of the human telomeric G-quadruplex [41]. However, it is controversial to explain the optical properties, such as hypochromicity and the shape and sign of CD bands [42]. Bates, et al. believed that a much better understanding of the various contributions to quadruplex CD spectra would be needed

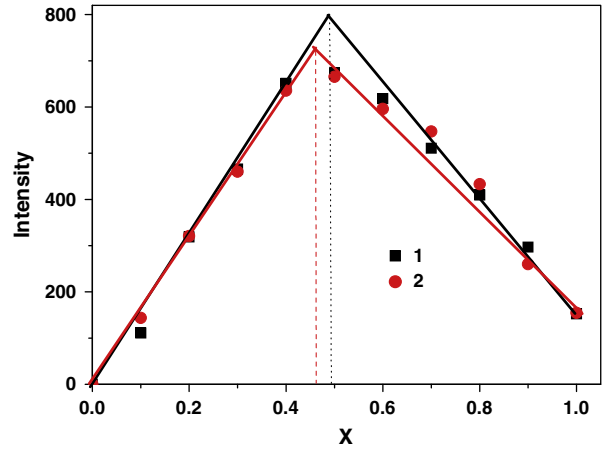

Fig. 5. Job plot using luminescence data for complexes 1 (■) and 2 (●) with a final G-quadruplex at 10.0 μM using a buffer solution of 100 mM KCl, 100 mM KH_2PO_4/Na_2HPO_4, and 1 mM K_2H_2EDTA with pH of 7.0. X = mole fraction of complex added to DNA.

before CD data were used alone to determine the structure of quadruplex molecular definitively when CD studies are useful in establishing the presence of quadruplex structures [42,43]. Fig. 6 shows the CD spectra of G-quadruplex at the absence or presence of two Ru(II) complexes. Upon addition of complexes 1 and 2 to the G-quadruplex aqueous solution, the maximum of absorbance at 290 nm was gradually suppressed and shifted to 285 nm. It implied that those two complexes have the tendency to form the anti-parallel conformation. The characteristic positive peak near 295 nm also supported the implication [44,45]. In addition, the conformation of G-quadruplex was not changed at a high ionic strength.

4. Conclusions

In this paper, we studied the interaction between two Ru(II) complexes and G-quadruplex. The results showed that complex 1 bound to the DNA more tightly than complex 2 did. Both complexes can induce the stabilization of quadruplex DNA. The ΔT_m were 9.4 and 7.0 at a [Ru]/[DNA] ratio of 1:1 for complexes 1 and 2, respectively. It implies that two complexes could be used as potential anticancer drugs. However, the conformation of G-quadruplex was not changed by the complexes at a high ionic strength in K^+ buffer. The details of the binding modes of these complexes with G-quadruplex and the structure of G-quadruplex are not clear yet and further studies are needed.

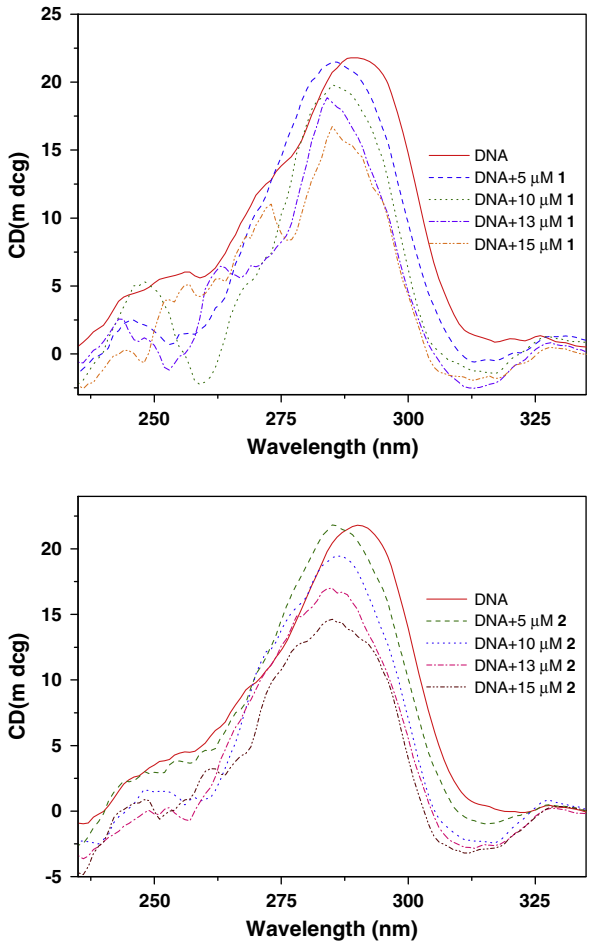

Fig. 6. CD spectra of G-quadruplex in the absence and presence of complexes 1 and 2, [DNA] = 5.0 μM, [Ru] = 0–15.0 μM.

Acknowledgements

We are grateful for financial support from the National Natural Science Foundation of China, the National Basic Research Program of China (973 Program No. 2007CB815306), and the Doctoral Program of Guangdong Medical College (B2009003).

Appendix A. Supplementary data

CCDC 782113 contains the supplementary crystallographic data for complexes 2. These data are free via http://www.ccdc.cam.ac.uk/conts/retrieving.html or from the Cambridge Crystallographic Data Centre. The contact information of the Centre is as follows: 12 Union Road, Cambridge CB2 1EZ, UK; fax: (+44) 1223-336-033; or e-mail: deposit@ccdc.cam.ac.uk.

Supplementary data to this article can be found online at doi:10.1016/j.jinorgbio.2010.10.005.

References

[1] M.A. Keniry, Biopolymers 56 (2001) 123–146.
[2] T. Simonsson, Biol. Chem. 382 (2001) 621–628.
[3] C.Y. Wei, G.Q. Jia, J.L. Yuan, Z.C. Feng, C. Li, Biochemistry 45 (2006) 6681–6691.
[4] J.E. Reed, A.J.P. White, S. Neidle, R. Vilar, Dalton Trans. (2009) 2558–2568.
[5] N.W. Kim, M.A. Piatyszek, K.R. Prowse, C.B. Harley, M.D. West, P.L. Ho, G.M. Coviello, W.E. Wright, S.L. Weinrich, J.W. Shay, Science 266 (1994) 2011–2015.
[6] J.W. Shay, S. Bacchetti, Eur. J. Cancer 33 (1997) 787–791.
[7] L.R. Kelland, Anticancer Drugs 11 (2000) 503–513.
[8] A.M. Burger, F. Dai, C.M. Schultes, A.P. Reszka, M.J. Moore, J.A. Double, S. Neidle, Cancer Res. 65 (2005) 1489–1496.
[9] V. Gabelica, E. Shammel Baker, M.P. Teulade-Fichou, E. De Pauw, M.T. Bowers, J. Am. Chem. Soc. 129 (2007) 895–904.
[10] A. Arora, C. Balasubramanian, N. Kumar, S. Agrawal, R.P. Ojha, S. Maiti, FEBS J. 275 (2008) 3971–3983.
[11] N.V. Anantha, M. Azam, R.D. Sheardy, Biochemistry 37 (1998) 2709–2714.
[12] D. Sun, B. Thompson, B.E. Cathers, M. Salazar, S.M. Kerwin, J.O. Trent, T.C. Jenkins, S. Neidle, L.H. Hurley, J. Med. Chem. 40 (1997) 2113–2116.
[13] OYu Fedoroff, M. Salazar, H. Han, V.V. Chemeris, S.M. Kerwin, L.H. Hurley, Biochemistry 37 (1998) 12367–12374.
[14] H. Mita, T. Ohyama, Y. Tanaka, Y. Yamamoto, Biochemistry 45 (2006) 6765–6772.
[15] H.Y. Han, D.R. Langley, A. Rangan, L.H. Hurley, J. Am. Chem. Soc. 123 (2001) 8902–8913.
[16] H. Bertrand, S. Bombard, D. Monchaud, M.P. Teulade-Fichou, J. Biol. Inorg. Chem. 12 (2007) 1003–1014.
[17] D.L. Ma, C.M. Che, S.C. Yan, J. Am. Chem. Soc. 131 (2009) 1835–1846.
[18] R. Kieltyk, J. Fakhoury, N. Moitessier, H.F. Sleiman, Chem. Eur. J. 14 (2008) 1145–1154.
[19] J. Talib, C. Green, K.J. Davis, T. Urathamakul, J.L. Beck, J.R. Aldrich-Wright, S.F. Ralph, Dalton Trans. (2008) 1018–1026.
[20] A.E. Friedman, J.C. Chambron, J.P. Sauvage, N.J. Turro, J.K. Barton, J. Am. Chem. Soc. 112 (1990) 4960–4962.
[21] A.E. Friedman, C.V. Kumar, N.J. Turro, J.K. Barton, Nucleic Acids Res. 19 (1991) 2595–2602.
[22] R.M. Hartshorn, J.K. Barton, J. Am. Chem. Soc. 114 (1992) 5919–5925.
[23] S. Shi, Xi.T. Geng, J. Zhao, T.M. Yao, C.R. Wang, D.J. Yang, L.F. Zheng, L.N. Ji, Biochimie 92 (2010) 370–377.
[24] C. Rajput, R. Rutkaite, L. Swanson, I. Haq, J.A. Thomas, Chem. Eur. J. 12 (2006) 4611–4619.
[25] J.H. Li, J.T. Wang, P. Hu, L.Y. Zhang, Z.N. Chen, Z.W. Mao, L.N. Ji, Polyhedron 27 (2008) 1898–1904.
[26] Y. An, Y.Y. Lin, H. Wang, H.Z. Sun, M.L. Tong, L.N. Ji, Z.W. Mao, Dalton Trans. (2006) 2066–2071.
[27] W. Paw, R. Eisenberg, Inorg. Chem. 36 (1997) 2287–2293.
[28] C.M. Dupureur, J.K. Barton, Inorg. Chem. 36 (1997) 33–43.
[29] G. Albano, P. Belser, C. Daul, Inorg. Chem. 40 (2001) 1408–1413.
[30] J. Sun, S. Wu, Y. Han, J. Liu, L.N. Ji, Z.W. Mao, Inorg. Chem. Commun. 11 (2008) 1382–1384.
[31] G.M. Sheldrick, SADABS 2.05, University of Göttingen, 2002.
[32] SHELXTL 6.10, Bruker Analytical Instrumentation, Madison, WI, USA, 2000.
[33] I. Haq, P. Lincoln, D. Suh, B. Norden, B.Z. Chowdhry, J.B. Chaires, J. Am. Chem. Soc. 117 (1995) 4788–4796.
[34] I. Haq, J.O. Trent, B.Z. Chowdhry, T.C. Jenkins, J. Am. Chem. Soc. 121 (1999) 1768–1779.
[35] L.M. Chen, J. Liu, J.C. Chen, C.P. Tan, S. Shi, K.C. Zheng, L.N. Ji, J. Inorg. Biochem. 102 (2008) 330–341.
[36] M.T. Carter, M. Rodriguez, A.J. Bard, J. Am. Chem. Soc. 111 (1989) 8901–8911.
[37] R.B. Nair, E.S. Teng, S.L. Kirkland, C.J. Murphy, Inorg. Chem. 37 (1998) 139–141.
[38] P.U. Maheswari, M. Palaniandavar, J. Inorg. Biochem. 98 (2004) 219–230.
[39] S. Shi, J. Liu, J. Li, K.C. Zheng, X.M. Huang, C.P. Tan, L.M. Chen, L.N. Ji, J. Inorg. Biochem. 100 (2006) 385–395.
[40] S. Shi, J. Liu, T.M. Yao, X.T. Geng, L.F. Jiang, Q.Y. Yang, L. Cheng, L.N. Ji, Inorg. Chem. 47 (2008) 2910–2912.
[41] P. Balagurumoorthy, S.K. Brahmachari, J. Biol. Chem. 269 (1994) 21858–21869.
[42] A.N. Lane, J.B. Chaires, R.D. Gray, J.O. Trent, Nucleic Acids Res. 36 (2008) 5482–5515.
[43] V. Đapić, V. Abdomerović, R. Marrington, J. Peberdy, A. Rodger, J.O. Trent, P.J. Bates, Nucleic Acids Res. 31 (2003) 2097–2107.
[44] D.P.N. Goncalves, R. Rodriguez, S. Balasubramanian, J.K.M. Sanders, Chem. Commun. (2006) 4685–4687.
[45] D.P.N. Goncalves, S. Ladame, S. Balasubramanian, J.K.M. Sanders, Org. Biomol. Chem. 4 (2006) 3337–3342.